applied sciences

MDPI

Article

The Influence of Headform/Helmet Friction on Head Impact Biomechanics in Oblique Impacts at Different Tangential Velocities

Óscar Juste-Lorente [1,*], Mario Maza [1], Mathieu Piccand [2] and Francisco J. López-Valdés [3]

[1] Impact Laboratory—Aragon Institute for Engineering Research (I3A), University of Zaragoza, 44600 Alcañiz, Spain; mmaza@unizar.es
[2] FIM (Fédération Internationale de Motocyclisme), Route de Suisse 11, 1295 Mies, Switzerland; mathieu.piccand@fim.ch
[3] Instituto de Investigación Tecnológica (IIT), ICAI Engineering School, Comillas Pontifical University, Alberto Aguilera, 23, 28015 Madrid, Spain; fjlvaldes@comillas.edu
* Correspondence: ojuste@unizar.es

Abstract: Oblique impacts of the helmet against the ground are the most frequent scenarios in real-world motorcycle crashes. The combination of two factors that largely affect the results of oblique impact tests are discussed in this work. This study aims to quantify the effect of the friction at the interface between the headform and the interior of a motorcycle helmet at different magnitudes of tangential velocity. The helmeted headform, with low friction and high friction surface of the headform, was dropped against three oblique anvils at different impact velocities resulting in three different magnitudes of the tangential velocity (3.27 m/s, 5.66 m/s, 8.08 m/s) with the same normal component of the impact velocity (5.66 m/s). Three impact directions (front, left-side and right-side) and three repetitions per impact condition were tested resulting in 54 impacts. Tangential velocity variation showed little effect on the linear acceleration results. On the contrary, the rotational results showed that the effect of the headform's surface depends on the magnitude of the tangential velocity and on the impact direction. These results indicate that a combination of low friction with low tangential velocities may result into underprediction of the rotational headform variables that would not be representative of real-world conditions.

Keywords: motorcycle helmet; oblique impact; tangential velocity; friction

Citation: Juste-Lorente, Ó.; Maza, M.; Piccand, M.; López-Valdés, F.J. The Influence of Headform/Helmet Friction on Head Impact Biomechanics in Oblique Impacts at Different Tangential Velocities. *Appl. Sci.* **2021**, *11*, 11318. https://doi.org/10.3390/app112311318

Academic Editor: Mariana Paulino

Received: 28 September 2021
Accepted: 25 November 2021
Published: 29 November 2021

1. Introduction

According to the World Health Organization, three hundred and seventy eight thousand people died in 2016 as a direct result of a motorcycle collision, amounting to 28% of the world's road traffic related deaths [1]. Despite the proven effectiveness of helmets in the protection of the head [2,3], head injuries are the leading cause of death and long-term disability after a motorcycle crash [4].

Traditionally, motor-vehicle related head injuries have been grouped according to the injury mechanism [5]. Since Holbourn hypothesized that rotational motion of the brain could explain some head injuries unlikely to be caused by translational motion [6], a substantial amount of research has supported the relationship between head rotation and brain injuries [7–9]. The reaction force that the helmeted head experiences in the contact against a rigid surface can be decomposed into two components: a normal component perpendicular to the impact surface and a tangential component parallel to the impact surface. The magnitude of the reaction force normal component is related mainly to the height of the rider's fall on the ground while the reaction force tangential component is associated to the motorcyclist's travelling speed [10]. The magnitude of this tangential component is directly related to the rotation experienced by the rider's head.

Oblique impacts between the helmet and the ground are the most frequent collision scenarios in real world [11,12]. Consequently, different laboratory testing protocols measure the helmet energy absorption capabilities and the resulting kinematics of a headform that represents the human head in oblique impacts [13–16].

Mills et al. identified the impact velocity component normal to the road, the friction coefficient between the shell and road, and the impact direction as the factors that control the peak headform rotational acceleration in oblique impacts [17–19]. Meng et al. showed that the impact velocity component normal to the road needs to be of a certain magnitude to induce the headform angular motion [20]. A follow-up study revealed that, from lower to higher tangential impact velocities, the motion of the helmet transitions from rolling to sliding, which affected head kinematics and its injury outcome for different friction values between the helmet and the ground [21]. However, the effective friction coefficient of the helmet as a whole is a function of the friction coefficient at the road/shell and at the head/liner interfaces [22]. Therefore, the tangential component of the contact force causes not only the rolling/sliding motion of the helmet on the ground but, due to similar underlying mechanics, it can also cause a relative motion between the head and the interior surface of the helmet [23].

To our knowledge, neither experimental nor computational studies have quantified the interaction of friction and tangential velocity in the resulting kinematics of the headform. Thus, the objective of this study is to quantify the influence of the friction between the interior surface of the helmet and the headform in the resulting kinematics of the headform at different magnitudes of the tangential impact velocity.

2. Methods

2.1. Experimental Design and Test Matrix

The experimental method was designed to identify the influence of the two proposed factors (friction and tangential velocity) and their interaction in four kinematically-based head injury predictors (outcome): the Peak of the resultant Linear Acceleration (PLA), the Head Injury Criterion (HIC) [24], the Brain Injury Criterion (BrIC) [25] and the Peak of the resultant Angular Acceleration (PAA).

A factorial analysis with two factors was independently applied to three different impact directions of the helmet and the anvil (front, right side and left side) in order to induce a rotation in each axis of the helmeted headform as shown in Figure 1. Only two friction conditions (low friction: bare headform; high friction: coated headform) were used at the interface between the headform and the interior of the helmet because friction showed a linear response on head angular kinematics [17]. However, three impact speeds (6.5 m/s, 8 m/s and 9.9 m/s) were selected because previous studies showed that varying the tangential velocity had a non-linear effect on head rotational kinematics [21]. These impact speeds were used with three different anvil angles (65°, 45° and 35°, respectively) so that while the tangential component of the impact speed changed, its normal component remained constant (see Figure A2). The values chosen for the friction and the impact speeds were based on the parameters prescribed in existing testing standard procedures [26,27].

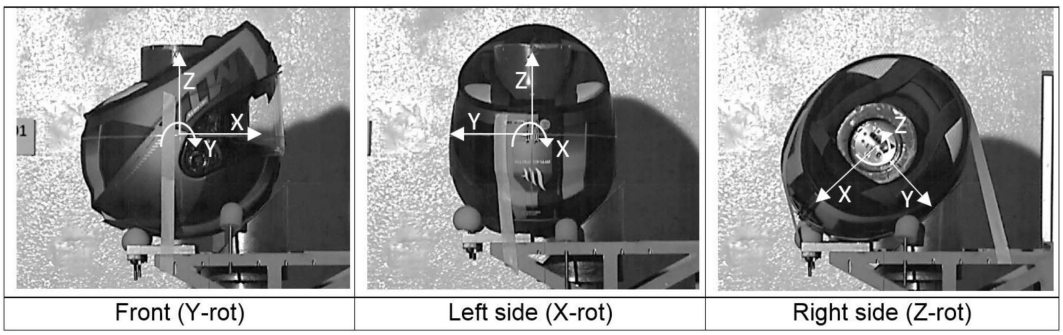

Figure 1. Oblique impact point layouts and coordinate system.

Thus, a 2 × 3 factorial design was chosen for each impact direction in which three replicas were carried out per each combination of levels of the selected factors, resulting in a total of 54 drop tests, as shown in Table 1.

Table 1. Test matrix. For N from 1 to 3, indicating repeated tests for a particular condition.

Resultant Impact Velocity	Anvil	Headform	Impact Point	Test ID
6.5 m/s	60°	Bare headform	Front (Y-rot)	DT0322-0N-01
			Left side (X-rot)	DT0322-0N-02
			Right side (Z-rot)	DT0322-0N-04
		Covered headform	Front (Y-rot)	DT0321-0N-01
			Left side (X-rot)	DT0321-0N-02
			Right side (Z-rot)	DT0321-0N-04
8.0 m/s	45°	Bare headform	Front (Y-rot)	DT0320-0N-01
			Left side (X-rot)	DT0320-0N-02
			Right side (Z-rot)	DT0320-0N-04
		Covered headform	Front (Y-rot)	DT0319-0N-01
			Left side (X-rot)	DT0319-0N-02
			Right side (Z-rot)	DT0319-0N-04
9.9 m/s	35°	Bare headform	Front (Y-rot)	DT0318-0N-01
			Left side (X-rot)	DT0318-0N-02
			Right side (Z-rot)	DT0318-0N-04
		Covered headform	Front (Y-rot)	DT0317-0N-01
			Left side (X-rot)	DT0317-0N-02
			Right side (Z-rot)	DT0317-0N-04

2.2. Testing Procedure

The tests were performed at the Impact Laboratory of the University of Zaragoza. A free fall guided impact machine (Model: Quebrantahuesos 6.0, +D, Pozuelo de Alarcón, Spain) was used for the drop tests. In the drop tests, the helmeted headform is placed on a carriage and restrained by pre-cut paper tape to prevent helmet motion during the fall. After releasing the carriage assembly from a specific height, the helmeted headform impacts the top surface of an anvil and the carriage assembly continues to fall onto a cushioned bed plate without interfering with the helmeted headform kinematics.

The helmet used was a full-face motorcycle helmet (model: FF104 RAPIDE, MT, Cartagena, Spain) (Figure A1). In total, 18 full face helmets of the M (57–58) size were used (using three impact locations per helmet, although each impact location on each helmet was tested just one time). The outer shell of the tested helmet was made of Fibre Reinforce Composite (FRC). The liner of the helmet was made of expanded polystyrene (EPS). The retention system of the helmet was based on a double D-ring buckle. The helmet complied with the United Nations Economic Commission for Europe (UNECE) regulation and Department of Transportation (DOT) standard.

The baseline case was a drop test performed at an impact velocity of 8.0 m/s onto a 45° oblique anvil, which originated two impact velocity components (normal and tangential) with the same magnitude of 5.66 m/s. The tangential velocity component (V_T) of this test set-up was altered approximately ±40%, while keeping constant the normal velocity component (V_N). Therefore, six helmets were drop tested at 6.5 m/s onto a 60° oblique anvil, obtaining a V_N of 5.66 m/s and a V_T of 3.27 m/s. Finally, six more helmets were

drop tested at 9.9 m/s onto a 35° oblique anvil to obtain the same V_N and a V_T of 8.08 m/s. These two test conditions are referred as −40% V_T and +40% V_T respectively (Figure A2).

The oblique anvils were made from a solid steel cylinder with the diameter of 130 mm. The impact surface of the anvil was covered with a sheet of grade 80 close-coat aluminium oxide abrasive paper, that was replaced after significant damage or after three impacts. There was not variation of the friction between the anvil surface and the exterior helmet surface. All the helmets were tested with a 575-size magnesium alloy full headform (Model: 100_04_FMH, Cadex Inc., Saint-Jean-sur-Richelieu, QC, Canada).

To vary the value of the friction between the interior of the helmet and the surface of the headform, half of the helmets per test condition were tested with the original metallic surface of the headform (bare headform) and half of them were tested with the headform covered with a uniform thin layer of high-performance silicone rubber (Model: Dragon Skin 10, Smooth-On, Inc., Macungie, PA, USA). A total of 40 g of silicone rubber was uniformly spread in order to meet the thickness requirement of the FRHPhe-01 standard [27]. A spring balance method was used to provide an indication of the friction associated to the coating treatment. The average coefficient of friction (COF) measured between a woven cotton fabric and the bare headform and the covered headform were 0.20 and 0.78, respectively.

The headform was positioned inside the helmets using a helmet positioning index (HPI) of 40 mm. The retention system was adjusted under the chin of the headform and tightened to a tension of 75 N [27]. Before each impact, the helmet was re-positioned and the retention system re-tensioned.

Three new helmet samples were used per each tangential velocity and headform surface condition. Each helmet was tested on front (Y-rot), left side (X-rot) and right side (Z-rot) (see Figure 1 for the position and orientation of the helmet coordinate system). The first impact was a frontal impact, leading to rotation in the sagittal plane around the *Y*-axis. The second impact was a parietal impact on the left side, leading to rotation in the frontal plane around the *X*-axis. In these two impacts, the central vertical axis (*Z*-axis) of the headform was aligned to the vertical. The third impact was a temporal impact on the right side, leading to rotation in the transverse plane around the *Z*-axis. For this oblique impact, the sagittal plane of the headform was positioned parallel to the impact surface of the anvil and the transverse plane of the headform was coincident with the vertical plane of symmetry of the anvil. Figure 1 shows the three oblique impact directions.

A wireless system (Model: iCONO, +D, Pozuelo de Alarcón, Spain) was used to measure linear acceleration and angular velocity at the centre of gravity of the headform. The wireless system incorporates three linear accelerometers (Model: 64C-2000, MEAS, Nanshan District Shenzhen, China), three angular rate sensors (Model: ARS PRO-8k, DTS, Seal Beach, CA, USA) and an acquisition system (Model: SLICE NANO, DTS, Seal Beach, CA, USA). Data were recorded at 10 kHz. Head linear acceleration signals were filtered using a low-pass filter CFC-1000 and angular velocities signals were filtered using a CFC-180. High-speed video was captured at 1000 Hz (Model: Eosens mini, Mikrotron, Unterschleissheim, Germany). The end of the impact was estimated when the measured acceleration was lower than 5 g, which correlated well with the instant in which the helmeted headform separated from the anvil. Data post-processing was performed using an in-house developed and validated script of Matlab (Matlab R2013b, MathWorks, Natick, MA, USA).

2.3. Data Analysis

Data were sorted first by impact direction (front, left side & right side), and then by the two factors: tangential velocity (−40% V_T, base case & +40% V_T) and headform friction condition (bare headform & covered headform). Thus, for each impact direction, a two-way analysis of variance (ANOVA) was used to estimate how each injury predictor changed according to the levels of tangential velocity and headform friction surface. The two-way ANOVA also checks for interactions between the two factors—for example, if the effect of the covered headform depends on the levels of the tangential velocities. When there

were not significant differences in the interaction, the one-way ANOVA and the Tuckey's HSD post-hoc test were performed to study each factor individually. In case of a significant interaction, the two-way ANOVA is transformed into a one-way ANOVA and the Tuckey's HSD post-hoc test was performed to study each possible combination between the two factors. Significance level used for all statistical tests was $\alpha = 0.05$. To increase the statistical power of the post-hoc tests that resulted in significant differences, only those comparisons with the largest effect sizes (as measured by Cohen's d) were considered in this study. Statistical analysis was performed using an Excel add-in (Real Statistics Resource Pack).

3. Results

3.1. Front Impact Kinematics

Figure 2 shows high-speed video captures at t = 14 ms, ilustrating the change in the angle between a reference line on the helmet shell (initially parallel to the horizontal direction) and a reference line on the neck of the headform, due to the relative motion between the helmet and the bare headform for each V_T. However, in the case of the high friction of the coated headform, the angle remained almost constant regardless of the V_T value.

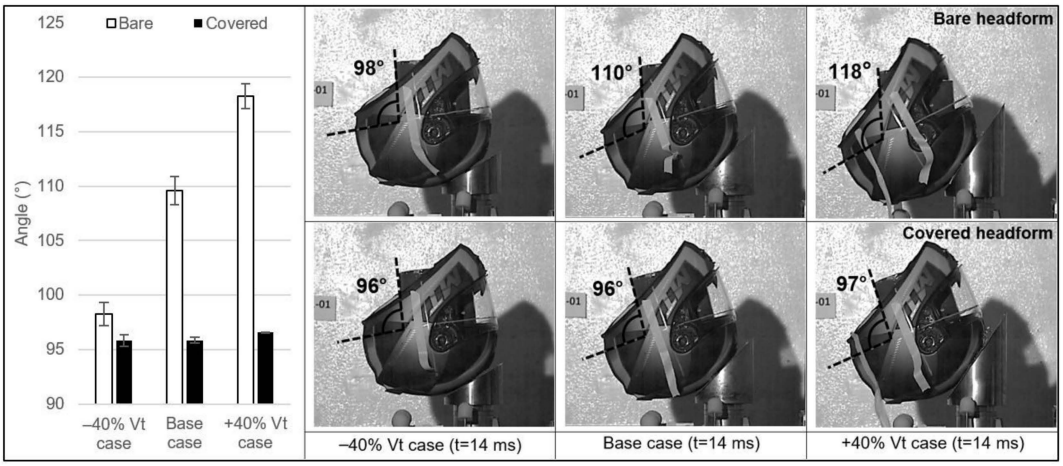

Figure 2. Comparison of the relative motion of the bare and covered headform inside the helmet at 14 ms of the front impact for each tangential velocity.

The comparison of the time history plots of the resultant linear acceleration is shown in Figure 3. The −40% V_T case (light grey traces) resulted in higher peak resultant linear acceleration and slightly shorter impact durations than the other two tangential velocities. This result might be influenced by the different location of the impact point between the helmet and the anvil, which was dependant on the tangential velocity component, as shown in Figure A3: reducing the magnitude of V_T shifted the impact point in the negative X direction. Within each value of V_T, the peak resultant acceleration of the high friction cases was consistently higher than the ones in the bare headform cases.

Figures 4 and 5 show the time history plot of the resultant angular velocity and the resultant angular acceleration. As expected, the influence of the magnitude of V_T in the angular velocity can be clearly identified in Figure 4. Regardless of the friction, the higher the magnitude of V_T, the higher the peak value of the angular velocity. Within each value of V_T, the coated headform (higher friction) resulted in higher magnitudes of angular velocity and a distinct maximum of the data trace, while the tests with the bare headform resulted in a monotonously growing curve.

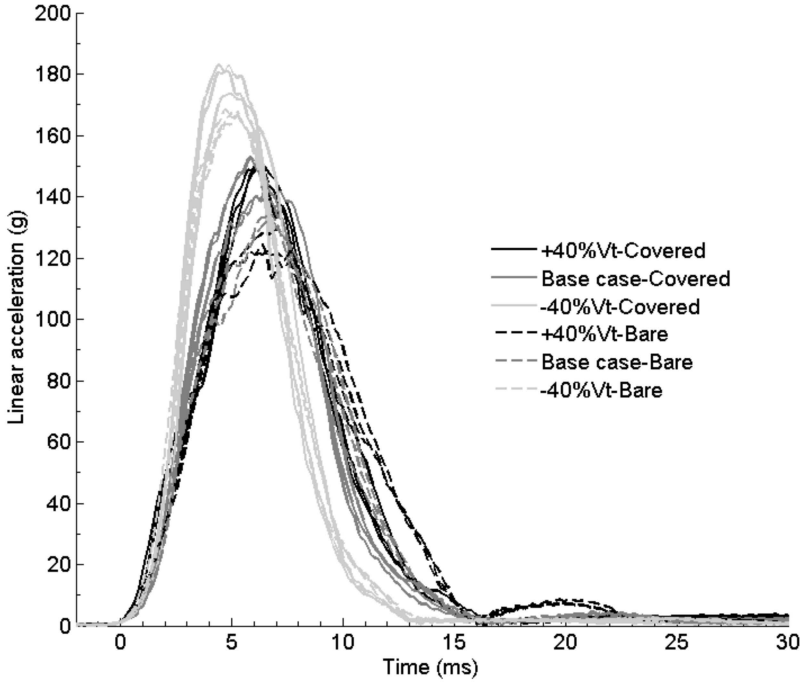

Figure 3. Time-history plot of the resultant linear acceleration for the front impacts. Solid lines correspond to covered headform and dashed lines correspond to bare headform test.

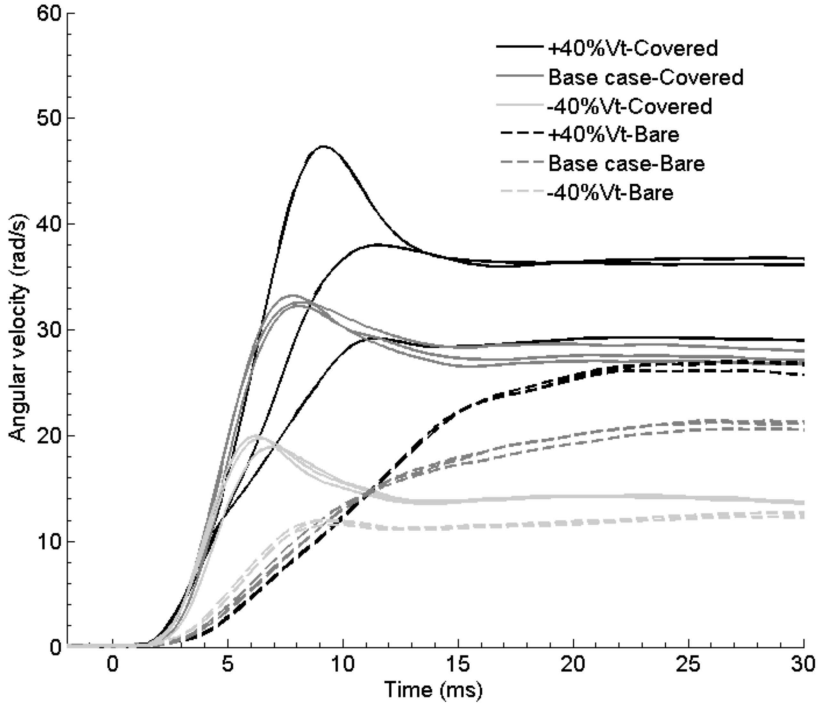

Figure 4. Resultant angular velocity for the front impacts. Solid lines correspond to covered headform and dashed lines correspond to bare headform test.

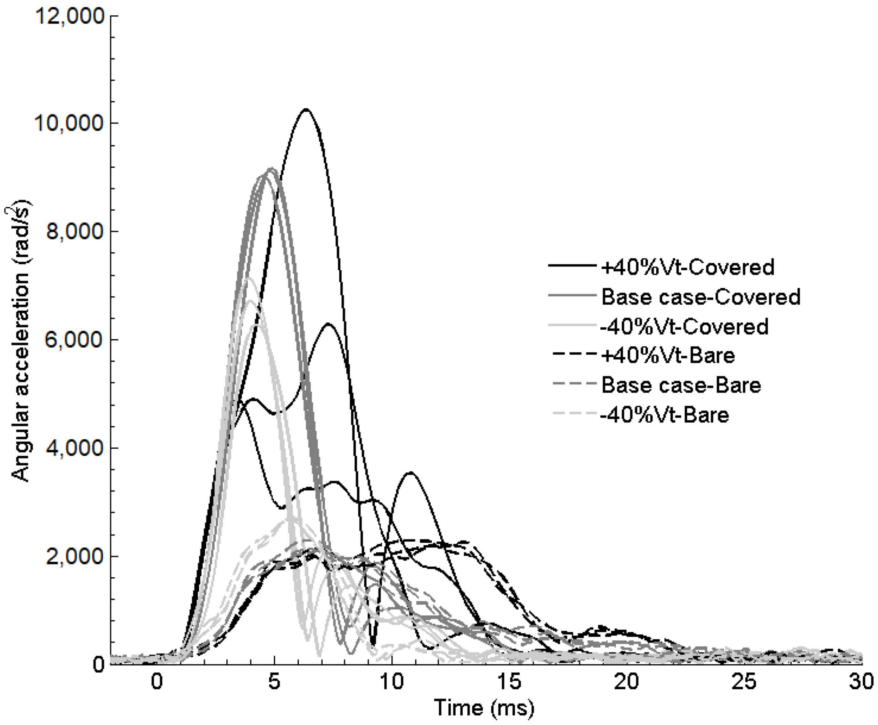

Figure 5. Resultant angular acceleration for the front impacts. Solid lines correspond to covered headform and dashed lines correspond to bare headform test.

The largest peak angular acceleration was obtained for one of the tests with the +40% V_T, while the other two repeats of the same condition resulted in two different responses and were comparable in peak magnitude to the −40% V_T cases (Figure 5). This lack of repeatability was attributed to the detachment of the helmet front vent in these two latter tests of the high friction tests. Note that these tests were not further included in the statistical analyses of the study. In the comparison between the baseline and the −40% V_T case, where there were not repeatability issues, the decrease in V_T is associated to a decrease in peak acceleration and shorter duration of the acceleration pulse. However, the peak angular acceleration did not show important differences between the different magnitudes of V_T while the duration of the acceleration pulse increased as the V_T increased in the low friction tests. Regardless the value of V_T, coating the headform with the silicone resulted in higher angular acceleration levels and shorter durations of the pulse, indicating a better coupling between the headform and the helmet.

3.2. Left Side Impact Kinematics

Figure 6 shows the high-speed video frames of the left-side impacts at t = 14 ms. Similarly to the previous configuration, the angle between a reference line on the helmet and the vertical central axis of the headform illustrated the relative motion between the helmet and the headform for each tangential velocity, that increased as the tangential velocity increased. In the +40% V_T case, when there was no additional room for the bare headform to move within the helmet, the shell of the helmet even deformed elastically. In the covered headform tests, the relative motion of the headform was reduced substantially.

No important differences were observed in the time history plots of the resultant linear acceleration (Figure 7) in left-side impacts: slightly lower peaks were observed in the lower friction tests, but the differences were not relevant.

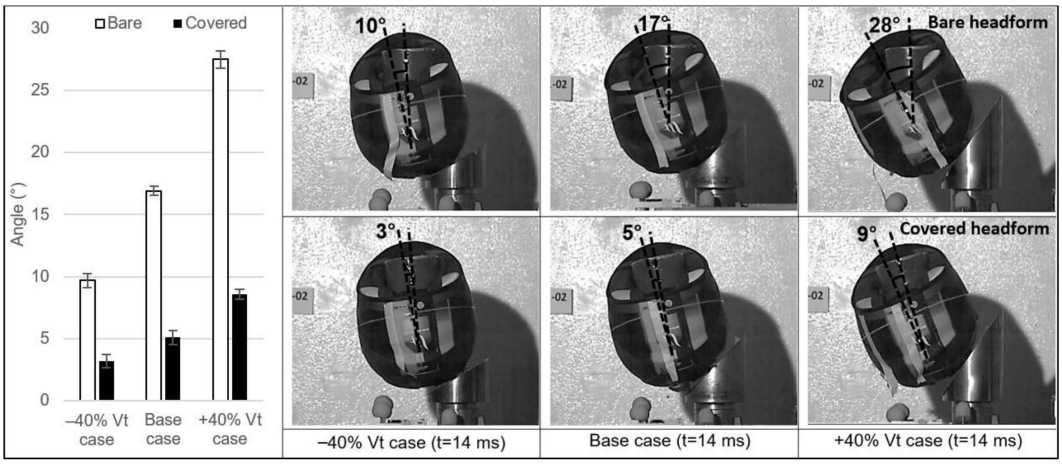

Figure 6. Comparison of the relative motion of the bare and covered headform inside the helmet at 14 ms of the left-side impact for each tangential velocity.

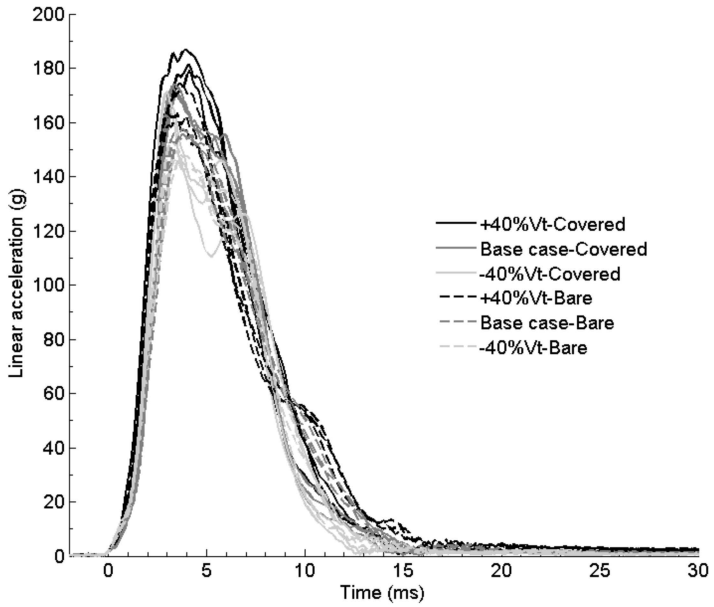

Figure 7. Resultant linear acceleration for the left side impacts. Solid lines correspond to covered headform and dashed lines correspond to bare headform test.

It is in the rotational behaviour of the headform where the differences began to arise. Figure 8 shows that the slopes of the traces corresponding to high friction are more similar than the slopes of the curves for the low friction at different magnitudes of V_T. As there was no relative motion between the headform and the helmet in the covered headform tests, the unique factor that influenced these slopes was the different magnitudes of V_T. On the contrary, in the bare headform tests, in which the relative motion increased as the V_T increased, there was a higher increase of the slopes of the curves as the magnitude of the tangential velocity increased resulting in that the +40% V_T slope was similar to the slopes of the high friction tests. This similitude at the highest V_T can be explained as the relative motion between the headform and the helmet is limited by the interaction of the geometry of the two solids. Higher values of V_T made this interaction to occur, and the headform and the helmet moved without relative motion increasing suddenly the slope and the magnitude of the angular velocity. Figure 9 shows completely different kinematics depending on the friction between the helmet and the headform: while the higher friction tests showed an initial global maximum and then a second local maximum, in the case of

the lower friction tests, the first maximum was local with the global maximum occurring about 8–10 ms later. The duration of the acceleration curve was longer also in the case of the lower friction tests. As for the influence of the magnitude of V_T, and independently of the value of the friction, higher values of V_T resulted in higher angular acceleration peaks.

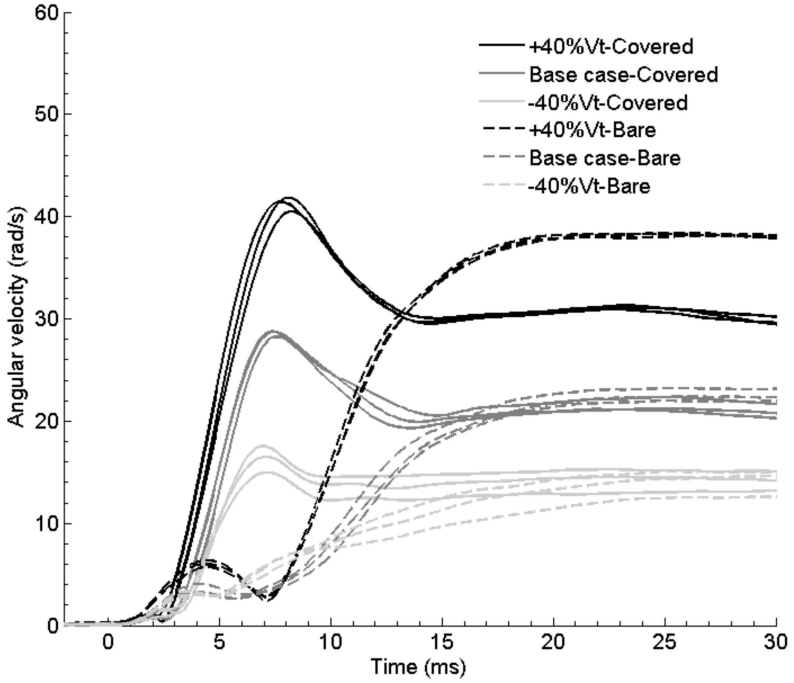

Figure 8. Resultant angular velocity for the left side impacts. Solid lines correspond to covered headform and dashed lines correspond to bare headform test.

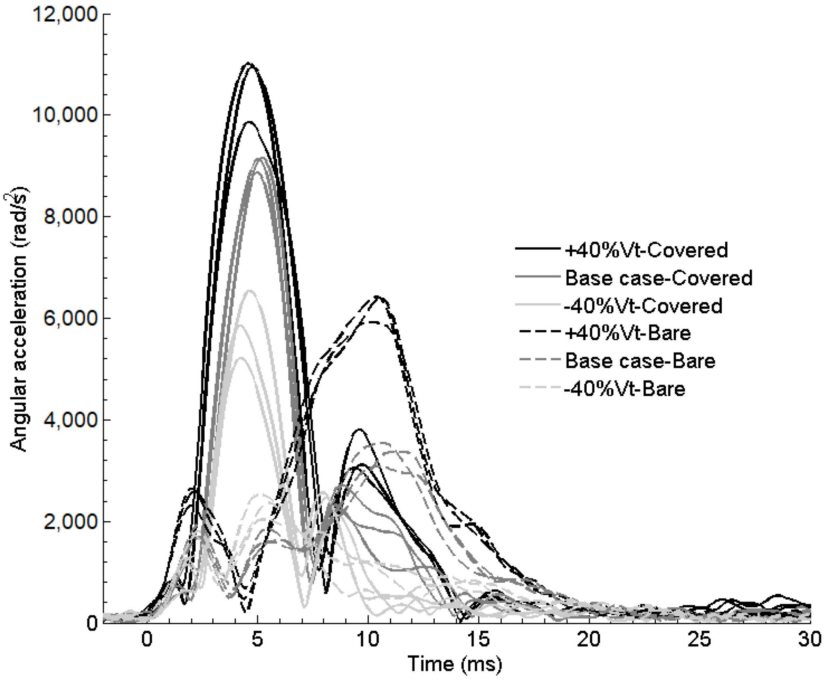

Figure 9. Resultant angular acceleration for the left side impacts. Solid lines correspond to covered headform and dashed lines correspond to bare headform test.

3.3. Right Side Impact Kinematics

Attending to the images from the high-speed video (Figure 10), it can be seen two different relative motions (indicated by the two dotted white lines in the Figure). The first one is a relative rotation around the *Z*-axis because of the tangential input applied to the helmet, which was mainly observed with the bare headform and increased as the V_T increased (illustrated by the angular misalignment of the two dotted white lines). The second one is a relative rotation around the *X*-axis because of the torque created by the distance from the impact point and the centre of gravity of the helmeted headform. It is observed with both headform friction conditions and remained almost constant for the different magnitudes of the V_T (illustrated by the parallel misalignment between the two dotted white lines).

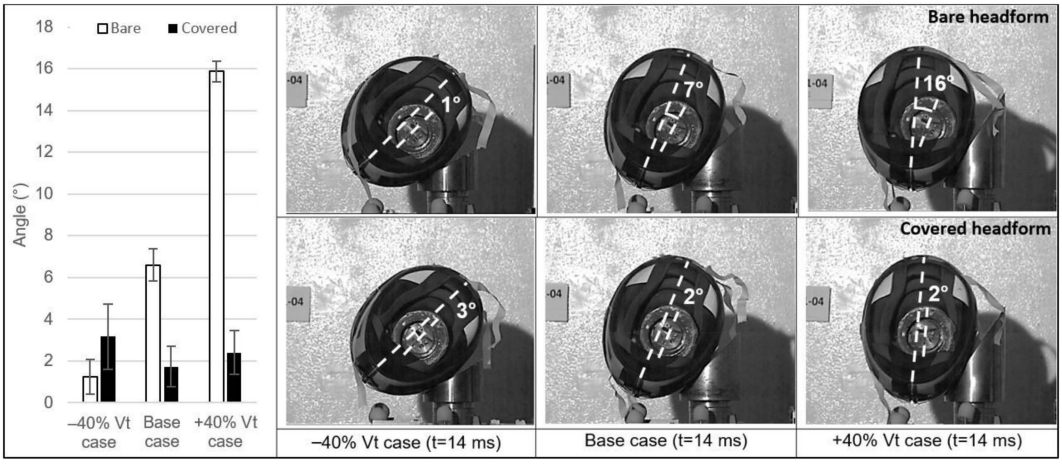

Figure 10. Comparison of the relative motion of the bare and covered headform inside the helmet at 14 ms of the right-side impact. Dashed lines indicate the headform position with respect to the helmet. The angle corresponds to the relative rotation around the *Z*-axis.

Similarly to the left-side impacts, the time history plot of the resultant linear acceleration did not show differences associated to either the magnitude of V_T or the friction condition (Figure 11).

Again, it is the rotational magnitudes the ones that were influenced by the change in these two parameters. The peak of the angular velocity was higher for higher values of V_T, independently of the friction condition (Figure 12). Increasing the friction between the helmet and headform resulted in a more identifiable angular velocity maximum, while the response of the bare headform produced slower increasing curve of the angular velocity, especially in the larger V_T cases. In the case of the angular acceleration, Figure 13 shows that higher values of V_T resulted in higher peaks of angular acceleration only when the headform was coated (high friction). When the friction was low (bare headform), no important differences were identified between the different values of V_T.

3.4. Data Statistical Analysis

The effect of the two factors and their interaction were analysed using a two-way ANOVA method for each injury predictor and each impact direction.

In addition, the post-hoc tests after the ANOVA allowed to quantify the effect of the headform surface treatment (bare vs. coated) for each level of the tangential velocity and the effect of the tangential velocity with respect to the base case level.

Regarding the peak of the resultant linear acceleration (PLA), there were significant differences in the effect of the coating factor for the front and left side impacts. The tangential velocity factor was significantly different for the three impact directions and the interaction term was not statistically significant at all (Table 2). Descriptive statistics of the test results and statistical results from the post-hoc tests for the PLA are presented in Table 3. Eight of the

eighteen PLA post-hoc comparisons resulted in significant differences (portrayed as shaded cells in Table 3). However, attending to the effect size only two comparisons (both in frontal impacts) were considered relevant: the increased PLA between the −40% V_T and baseline for the bare headform (167 ± 1 g vs. 135 ± 3 g) and the increased PLA between the −40% V_T and baseline for the covered headform (180 ± 5 g vs. 149 ± 6 g).

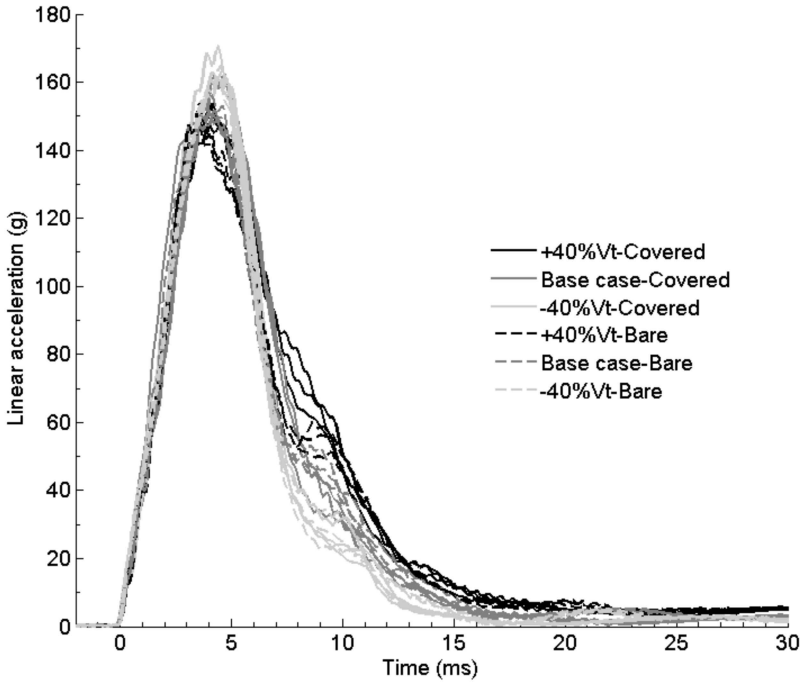

Figure 11. Resultant linear acceleration for the right side impacts. Solid lines correspond to covered headform and dashed lines correspond to bare headform test.

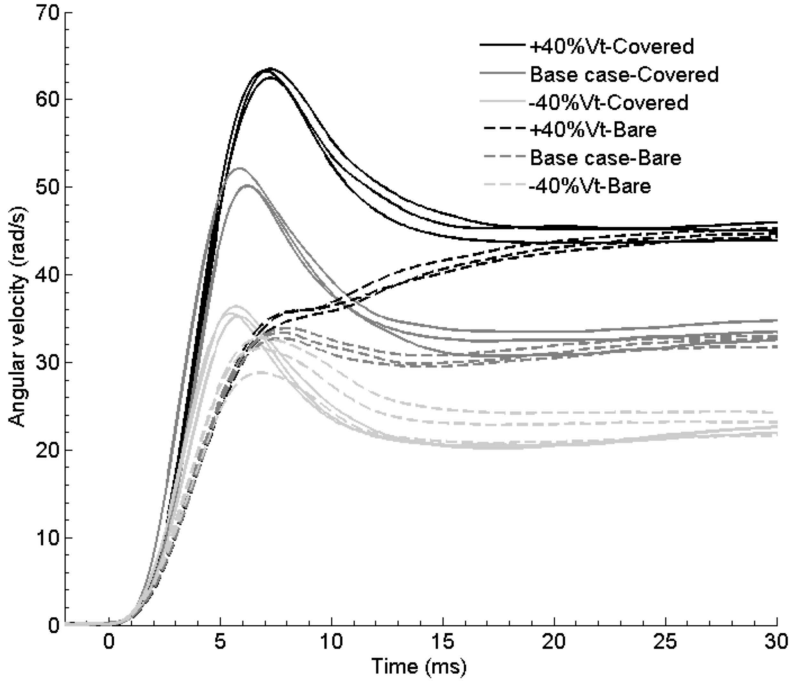

Figure 12. Resultant angular velocity for the right side impacts. Solid lines correspond to covered headform and dashed lines correspond to bare headform test.

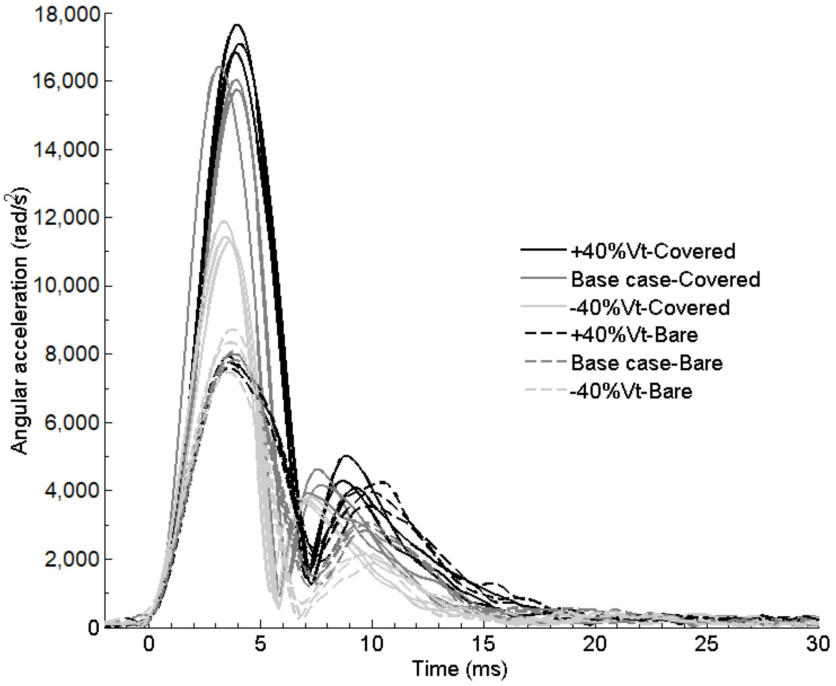

Figure 13. Resultant angular acceleration for the right side impacts. Solid lines correspond to covered headform and dashed lines correspond to bare headform test.

Table 2. Two-way ANOVA results (*p*-values) for the PLA. *p*-values < 0.05 portrayed as shaded cells.

	Front (Y-Rot)	Left Side (X-Rot)	Right Side (Z-Rot)
Coating	0.0005	0.00016	0.11161
Tangential velocity	1.37×10^{-6}	0.00095	0.00031
Interaction	0.72203	0.99408	0.73341

Table 3. Averages, standard deviation (SD), coefficient of variation (CV) and post-hoc results for PLA. *p*-values < 0.05 portrayed as shaded cells.

	PLA (g)		Front (Y-Rot)			Left Side (X-Rot)			Right Side (Z-Rot)		
			−40% V_T	Base Case	+40% V_T	−40% V_T	Base Case	+40% V_T	−40% V_T	Base Case	+40% V_T
Bare headform	Average		167	135	125	149	156	167	163	153	149
	SD		1	3	4	3	1	6	2	3	4
	CV(%)		0.64%	2.59%	2.90%	2.19%	0.73%	3.50%	1.28%	1.89%	2.40%
	V_T effect	Cohen's d	6.43	—		1.41	2.21		2.01	0.80	
		p-value	0.00011	—		0.12211	0.03969		0.01523	0.38922	
Covered	Average		180	149	150	164	172	182	165	158	151
	SD		5	6	0	13	2	4	5	6	3
	CV(%)		2.98%	3.70%	0.25%	7.78%	1.23%	2.16%	3.09%	3.67%	2.09%
	V_T effect	Cohen's d	6.23	—		1.61	2.01		1.41	1.41	
		p-value	0.00239	—		>0.05	>0.05		0.27546	0.27695	
Coating effect		Cohen's d	2.61	2.81	—	3.01	3.22	3.01	0.40	1.00	0.40
		p-value	0.01592	0.00186	—	0.11458	0.00032	0.01765	>0.05	>0.05	>0.05

Concerning the head injury criterion (HIC), there were significant differences for the coating and the tangential velocity factors for the three impact directions (see Table 4). The interaction between the factors was significant in the left and right-side impacts. Nine of

the eighteen HIC post-hoc comparisons resulted in significant differences but attending to the effect size (Cohen's d), only five were considered relevant (Table 5). The identified relevant differences were the following: the increased HIC between the −40% V_T and base case for the bare headform (1213 ± 30 vs. 870 ± 11) and covered headform (1382 ± 25 vs. 1058 ± 12) in the front impact; the decreased HIC between the −40% V_T and base case for the covered headform (1099 ± 116 vs. 1378 ± 11) in the left side impact; and the decreased HIC between the bare and covered headform for the base case (1056 ± 20 vs. 1378 ± 11) and for the +40% V_T case (1145 ± 68 vs. 1552 ± 102) in the left side impact.

Table 4. Two-way ANOVA results (*p*-values) for the HIC. *p*-values < 0.05 portrayed as shaded cells.

	Front (Y-Rot)	**Left Side (X-Rot)**	**Right Side (Z-Rot)**
Coating	5.23×10^{-7}	7.42×10^{-6}	2.45×10^{-7}
Tangential velocity	3.76×10^{-9}	0.00012	0.00692
Interaction	0.45659	0.00319	0.04017

Table 5. Averages, standard deviation (SD), coefficient of variation (CV) and post-hoc results for HIC. *p*-values < 0.05 portrayed as shaded cells.

	HIC		**Front (Y-Rot)**			**Left Side (X-Rot)**			**Right Side (Z-Rot)**		
			−40% V_T	**Base Case**	**+40% V_T**	**−40% V_T**	**Base Case**	**+40% V_T**	**−40% V_T**	**Base Case**	**+40% V_T**
Bare headform	Average		1213	870	857	1049	1056	1145	893	825	781
	SD		30	11	15	58	20	68	32	15	16
	CV(%)		2.51%	1.31%	1.73%	5.53%	1.86%	5.98%	3.64%	1.81%	2.10%
	V_T effect	Cohen's d	6.93	—		0.14	1.80		1.37	0.89	
		p-value	0.00005	—		0.99999	0.68434		0.10190	0.46244	
Covered	Average		1382	1058	947	1099	1378	1552	953	949	936
	SD		25	12	47	116	11	102	39	30	32
	CV(%)		1.82%	1.13%	4.96%	10.56%	0.83%	6.59%	4.04%	3.11%	3.47%
	V_T effect	Cohen's d	6.54	—		5.63	3.51		0.08	0.26	
		p-value	0.00004	—		0.00576	0.10668		0.99995	0.99216	
Coating effect		Cohen's d	3.41	3.80	—	1.01	6.50	8.22	1.21	2.50	3.13
		p-value	0.00179	0.00004	—	0.95603	0.00184	0.00022	0.18190	0.00204	0.00028

Regarding BrIC, the two-way ANOVA resulted in significant differences for the two factors and their interaction in the three impact configurations (Table 6). All BrIC post-hoc comparisons were statistically significant (Table 7). The effect size revealed significant differences for all comparisons. Due to the magnitude of the effect size, it is worth highlighting the differences between the baseline case and the +40 V_T case for the bare headform in the left side impact (0.280 ± 0.008 vs. 0.540 ± 0.002) and in the right-side impact (0.750 ± 0.007 vs. 1.060 ± 0.015).

Table 6. Two-way ANOVA results (*p*-values) for the BrIC. *p*-values < 0.05 portrayed as shaded cells.

	Front (Y-Rot)	**Left Side (X-Rot)**	**Right Side (Z-Rot)**
Coating	6.14×10^{-11}	2.86×10^{-10}	1.73×10^{-12}
Tangential velocity	2.78×10^{-10}	1.61×10^{-14}	6.35×10^{-14}
Interaction	4.60×10^{-7}	0.00131	9.13×10^{-7}

Table 7. Averages, standard deviation (SD), coefficient of variation (CV) and post-hoc results for BrIC. *p*-values < 0.05 portrayed as shaded cells.

BrIC			Front (Y-Rot)			Left Side (X-Rot)			Right Side (Z-Rot)		
			−40% V_T	Base Case	+40% V_T	−40% V_T	Base Case	+40% V_T	−40% V_T	Base Case	+40% V_T
Bare headform	Average		0.210	0.310	0.400	0.170	0.280	0.540	0.620	0.750	1.060
	SD		0.004	0.007	0.001	0.020	0.008	0.002	0.040	0.007	0.015
	CV(%)		1.88%	2.35%	0.27%	11.88%	2.78%	0.43%	6.54%	0.98%	1.44%
	V_T effect	Cohen's d	6.15	—		6.76	15.99		7.99	19.06	
		p-value	1.02×10^{-6}	—		2.46×10^{-6}	2.86×10^{-10}		9.23×10^{-5}	1.03×10^{-8}	
Covered	Average		0.350	0.580	0.680	0.260	0.440	0.630	0.770	1.140	1.430
	SD		0.011	0.008	0.158	0.022	0.002	0.010	0.013	0.029	0.004
	CV(%)		3.03%	1.33%	23.25%	8.47%	0.49%	1.63%	1.73%	2.51%	0.30%
	V_T effect	Cohen's d	14.14	—		11.07	11.68		22.75	17.83	
		p-value	2.03×10^{-9}	—		1.32×10^{-8}	6.84×10^{-9}		1.15×10^{-9}	1.95×10^{-8}	
Coating effect		Cohen's d	8.61	16.6	—	5.53	9.84	5.53	9.22	23.98	22.75
		p-value	9.96×10^{-8}	9.29×10^{-10}	—	1.95×10^{-5}	5.14×10^{-8}	1.21×10^{-5}	3.24×10^{-5}	7.58×10^{-10}	1.21×10^{-9}

Finally, significant differences of the two-way ANOVA for the peak of the resultant angular acceleration (PAA) were found both for the coating factor, the magnitude of the tangential velocity and their interaction in all three impact directions (Table 8). In this case, all post-hoc comparisons for the covered headform resulted in significant differences and the effect size revealed strong differences in most cases. On the contrary, in the case of the bare headform, only one comparison for the tangential velocity with the bare headform resulted in significant differences (Table 9). This comparison was between the base case and the +40% V_T case in the left side impact (3330 ± 233 rad/s^2 vs. 6241 ± 277 rad/s^2).

Table 8. Two-way ANOVA results (*p*-values) for the PAA. *p*-values < 0.05 portrayed as shaded cells.

	Front (Y-Rot)	Left Side (X-Rot)	Right Side (Z-Rot)
Coating	1.10×10^{-10}	3.02×10^{-11}	4.61×10^{-14}
Tangential velocity	0.00009	2.43×10^{-9}	9.12×10^{-8}
Interaction	3.56×10^{-6}	0.00280	2.04×10^{-8}

Table 9. Averages, standard deviation (SD), coefficient of variation (CV) and post-hoc results for PAA. *p*-values < 0.05 portrayed as shaded cells.

PAA (rad/s^2)			Front (Y-Rot)			Left Side (X-Rot)			Right Side (Z-Rot)		
			−40% V_T	Base Case	+40% V_T	−40% V_T	Base Case	+40% V_T	−40% V_T	Base Case	+40% V_T
Bare headform	Average		2681	2168	2241	2305	3330	6241	8171	7955	7753
	SD		14	101	51	248	233	277	641	127	166
	CV(%)		0.51%	4.66%	2.26%	10.76%	7.01%	4.43%	7.84%	1.60%	2.15%
	V_T effect	Cohen's d	1.41	—		2.82	8.00		0.59	0.55	
		p-value	0.08917	—		0.09604	2.56×10^{-5}		0.97741	0.98343	
Covered	Average		6702	9106	7141	5864	9050	10607	11524	16055	17173
	SD		433	70	2778	663	161	646	308	339	421
	CV(%)		6.46%	0.77%	38.90%	11.30%	1.78%	6.09%	2.67%	2.11%	2.45%
	V_T effect	Cohen's d	6.60	—		8.75	4.28		12.45	3.07	
		p-value	5.20×10^{-6}	—		1.00×10^{-5}	0.00729		5.39×10^{-8}	0.03035	
Coating effect		Cohen's d	11.05	19.06	—	9.78	15.71	12.00	9.21	22.25	25.88
		p-value	9.34×10^{-8}	1.81×10^{-9}	—	3.08×10^{-6}	1.50×10^{-8}	3.26×10^{-7}	1.55×10^{-6}	6.99×10^{-11}	7.61×10^{-12}

4. Discussion

This study investigated the combined effect of the friction force between the interior surface of the helmet and the headform and different tangential velocities in helmet oblique impacts. The experimental data included in this manuscript are particularly relevant to design helmet oblique testing protocols capable of including real-world like characteristics. The data gathered here highlight the importance of the interaction between the friction between the head and the helmet and the tangential velocity in the resulting kinematics of the head.

4.1. The Variability of the Friction between the Human Skin and the Helmet Inner Liner

Human skin has been shown to exhibit a complex and highly variable friction behaviour. Ebrahimi et al. obtained an average friction coefficient between the interior of the helmet (nylon fabric) and the human skin of 0.683 [23]. However, other experiments using human cadaver heads estimated substantially lower values for the coefficient of friction between the interior of the helmet (polyester fabric, a common material used in the interior liner of helmets) and the scalp (0.29 ± 0.07) [28]. In a tactile perception study unrelated to helmets, Ramalho et al. reported a COF about 0.7 between polyester fabric and the volar forearm of in vivo volunteers [29]. This value could be even higher in the case of the head, as other experimental studies have revealed that friction coefficients at the volar forearm were lower (COF = 0.26) than those measured on the forehead (COF = 0.34) [30]. The variation of friction coefficients measured for the human skin has been suggested to depend on skin hydration [31], with moisture increasing the value of the COF between the skin and the fabric up to a maximum and then decreasing it, when there is excess of water in the interface [31,32]. As sweating is very common among helmeted riders specially in warmer weathers, this study is essential to understand how the performance of helmets can be affected by changes in the COF.

Although the influence of the COF had been addressed already in [23], to our knowledge, this is the first time that an experimental study combines the effect of varying the tangential component of the impact velocity and the COF at the same time. Our data shows

that the combination of different magnitudes of V_T and of COF influences differently the helmet performance.

4.2. Linear Acceleration-Based Injury Predictors

The experimental results included here regarding the V_T variation are consistent with two computational studies which concluded that the influence of increasing tangential velocity on the linear acceleration is insignificant [17,21]. In the right-side impacts, where the impact point was the same for the three tangential velocities, the PLA and HIC magnitudes decreased slightly as the tangential velocity increased (Figure 11). This slight decrease can be explained by an increased helmet rotation caused by higher values of V_T, which could bring new areas of uncrushed liner into the impact area, contributing to the decrease of PLA and HIC magnitudes [33].

It is true that in the front and left side impact directions the statistical analyses resulted in significant differences for the PLA and HIC magnitudes. However, for these impact directions, the central vertical axis (*Z*-axis) of the headform was aligned to the vertical and, consequently, the impact point location changed with the angle of the anvil (see Figure A3). PLA and HIC magnitudes decreased as the V_T increased in the front impacts while they increased as the tangential velocity increased in the left side impact direction. This opposite trend suggests that these differences are due to the variation of the impact point location and not due to the change in V_T.

Regarding the coating effect, the PLA and HIC magnitudes obtained were always higher for the tests with high friction. The relative motion of the headform in the helmet, which depends on the tangential velocity for the bare headform, modified the crushing liner area depending on the geometry of the headform close to the impact point. Therefore, depending on the liner density around the impact point and the crushing liner area variation, the PLA and HIC could decrease, remain constant or even increase. This is supported by Ebrahimi et al., that found that the average linear acceleration of the headform with the highest friction for the 15° anvil decreased by 26% while it increased by 10% for the 30° anvil [23].

4.3. Angular Motion-Based Injury Predictors

The significance of the interaction of the two analysed factors in the two-way ANOVA for the two angular injury predictors showed that the effect of the friction depends on the magnitude of the tangential velocity. This dependence of the friction effects with the V_T is mainly due to the combination of the rolling and sliding phenomena at the helmet/anvil interface, which was observed in the high friction tests and it was studied in detail by Meng et al. [21] and to the relative motion between the headform and the helmet, which was observed in the low friction tests.

In the case of the coated headform, brain injury criterion (BrIC) and peak of the resultant angular acceleration (PAA) increased as the tangential velocity increased for the three impact directions. Interestingly, our experiments showed that the relative increase of the angular injury predictors was higher from the −40% V_T case to the base case than from the base case to the +40% V_T case. As demonstrated in Meng et al., the effect of increasing V_T in the rotation of the helmet is negligible once the helmet is sliding [21]. This suggest that from −40% V_T case to the base case the helmets were in rolling phase while from base case to the +40% V_T case the helmets were in the transition phase from rolling to sliding.

In the bare headform tests, BrIC also increased as the V_T increased but PAA did not in the front and right-side directions, in which PAA were almost constant. In this case, in which the helmet was also rolling on the anvil for lower values of V_T as in the case of the coated headform, the lower friction between the headform and the helmet caused the bare headform to slide inside the helmet. This sliding motion limited the maximum angular acceleration (slope of the angular velocities curves) but not the maximum angular velocity, which also depends on the duration of the angular acceleration, which was higher for the higher V_T values (see Figure 5). In the left side impacts, the relative motion of the headform inside the helmet was prevented by the interaction of the geometry of the headform and

the geometry of the helmet, as the V_T increased. In the +40% V_T case, the relative motion came to an end and helmet and headform moved jointly increasing the headform rotational motion significantly.

4.4. Implications for Helmet Testing Programs

The existing interaction of the friction between the helmet and the headform and V_T needs to be recognized when a testing program is being planned. Existing helmet testing methods have been shown to use speeds which are lower than those found in real world situations, mainly due to limitation of the height of the helmet drop facilities of the testing laboratories [21]. This implies lower magnitude for the tangential component of the velocity than those found in real world situations. Therefore, on top of the underestimation caused by a lower tangential velocity, there may be an additional underestimation of the rotational motion of the head if the friction between the headform and the helmet is low and, consequently, the headform slides inside the helmet without being stopped by the interaction between the geometries of the headform and the helmet. As discussed above, there is evidence showing that the friction coefficient between the human head and the liner of the helmet can be around 0.7. This friction is expected to increase if there is sweating, which can be common especially in warm weathers [32]. Thus, as several existing testing programs are starting to investigate different injury metrics related to the rotation of the headform and these programs should be looking into testing the helmets so that they are effective in a worst-case (but possible) scenario, our study suggests that the friction at the interface helmet/headform in oblique helmet programs should be high enough to guarantee the joint motion of the unit without sliding of the headform.

In addition, most helmet standards call for helmets to be tested in linear impacts (without tangential component) at the highest levels of severity ignoring the helmet response to lower severity impacts. Recently, some helmet standards such as FRHPhe-01 [27] and ECE 22.06 [26] included a low severity linear impact test at 5 m/s and 6 m/s respectively in their test methods in order to avoid that helmets transmit unacceptably high levels of linear acceleration in low severity impact events. Beside of these low severity impact tests, these standards also include an oblique impact test at 8.0 m/s against a 45-degree anvil, which originate two impact velocity components (normal and tangential) with the same magnitude of 5.66 m/s. This study supports that the oblique impact test also included in these helmet standards could be sufficient to characterize the linear acceleration in low severity impacts without the need of a specific low severity test. Since the influence of the V_T on the linear acceleration is insignificant and the magnitude of the normal component of the impact velocity of the oblique test (5.66 m/s) is already within the range of the low-speed tests recently included in the aforementioned standards.

4.5. Limitations of the Study and Future Work

As aforementioned, the high-speed video analysis revealed that the front vent of the helmet was detached during the impact in two of the three replicas of the +40% V_T case with the headform covered. This fact was the cause of the low repeatability obtained for the angular velocity and angular acceleration in the mentioned condition. In consequence, these tests were not considered in the statistical analysis.

The rigid magnesium EN960 headforms do not have an outer layer to simulate the scalp tissue or hair because they are not designed to respond like a human head to impact. Therefore, slippage between the scalp and skull, the effect of the hair (which could reduce the head/helmet friction) and the tensioning effect of the skin were not covered in this work [33,34]. Even if a study identified that scalp tissue affects head biomechanics in a significant way [28], it also concluded that the friction coefficient of the outer layer of the headform and the interaction with the helmet reduced the relative effect of the scalp.

The influence of the neck and body in the kinematics of the headform was not included in this study. Several studies suggest that the neck and body play only a small role during helmeted head impacts [35,36] whereas other studies suggest that the presence of the neck

and body have a significant influence on head kinematics and that it is strongly dependent on the impact configuration [37,38]. Isolated head surrogate was used in this study due to its simplicity and because this is the condition used in the European helmet testing regulation [26].

Despite tissue-based metrics such as Maximum Principal Strain (MPS) are desirable for assessing brain injury risk since they are a measure of the primary injury mechanism, this study looked only into four kinematic-based metrics (PLA, HIC, BrIC and PAA). These were the parameters that could be obtained directly from test measurements. In addition, BrIC has been shown to have a good correlation with several tissue-based metrics in a bicycle helmet study [39].

Another limitation of this work is that only one full-face helmet model and three impact directions were tested. Therefore, the results of this study may vary for other helmet types and other impact directions. Future research should investigate the friction between different materials used as comfort padding and the human scalp, considering the physiological skin condition and the effect of sweat.

5. Conclusions

This study has evaluated the effect of the friction of the headform and the interior surface of the helmet in oblique impacts at different tangential velocities. As oblique testing helmet programs specify a friction in the contact between the headform and the interior surface of the helmet, the value of this friction needs to be chosen carefully. Since the influence of the friction depends on the magnitude of the tangential velocity, the magnitude of these two factors must be chosen jointly. The results of our experiments show that the combination of low friction with lower speeds that the ones occurring in real-world crashes may result into underprediction of the rotational headform variables that would not be representative of real-world conditions, in which a higher V_T or the sweat of the rider's head would increase the rotational motion experienced by the rider's head.

It has also been shown experimentally that the influence of increasing tangential velocity on the linear acceleration measured by the headform is negligible. Therefore, oblique testing programs including a normal component of the impact velocity that represents a low severity impact would assess if helmets may transmit unacceptably high levels of linear acceleration even in low severity impact events.

Author Contributions: Conceptualization, F.J.L.-V. and Ó.J.-L. and Ó.J.-L.; Methodology, Ó.J.-L.; Software, Ó.J.-L.; Validation, Ó.J.-L.; Formal Analysis, Ó.J.-L.; Investigation, F.J.L.-V., M.M. and Ó.J.-L.; Resources, M.M.; Data Curation, Ó.J.-L.; Writing—Original Draft Preparation, Ó.J.-L.; Writing—Review & Editing, F.J.L.-V. and Ó.J.-L.; Visualization, F.J.L.-V.; Supervision, Ó.J.-L.; Project Administration, M.M. and Ó.J.-L.; Funding Acquisition, M.M. and M.P. All authors have read and agreed to the published version of the manuscript.

Funding: This research received no external funding.

Institutional Review Board Statement: Not applicable.

Informed Consent Statement: Not applicable.

Data Availability Statement: Experimental data can be available for non-commercial purposes under request. Please contact: ojuste@unizar.es.

Acknowledgments: The authors would like to thanks the collaboration of the FIM (Fédération Internationale de Motocyclisme) for supporting this work partially and Víctor Lasmarias for his assistance during the tests.

Conflicts of Interest: The authors declare no conflict of interest.

Appendix A. Helmet Model, Impact Velocities Diagram and Impact Point Locations

Figure A1. MT FF104 RAPIDE full-face helmet.

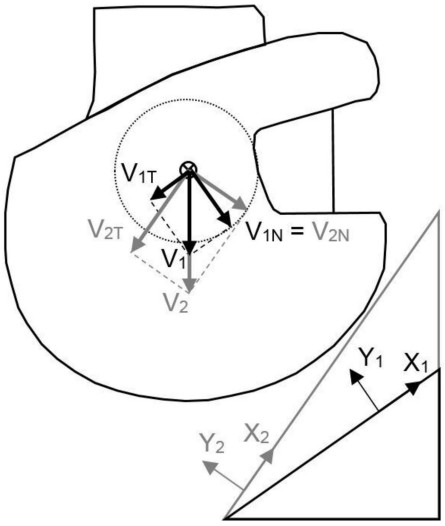

Figure A2. Impact velocities diagram. Modifying the angle of the anvil and the impact speed, the tangential component of the impact velocity can be modified keeping the magnitude of the normal component.

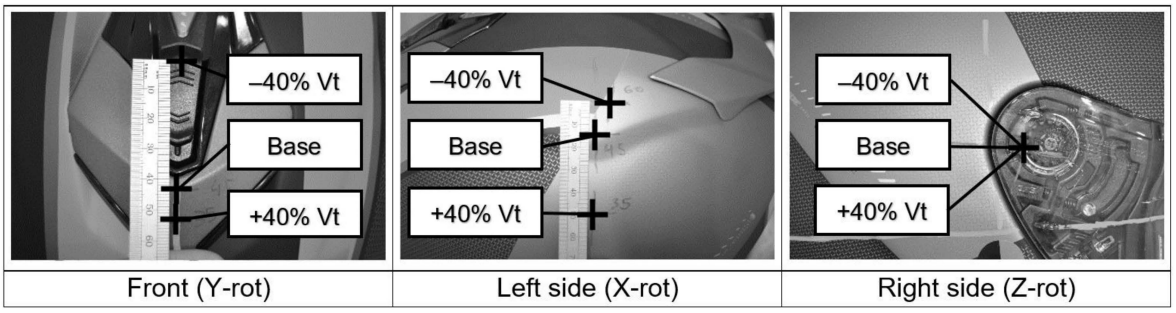

Figure A3. Impact point locations for each impact layout and tangential velocity.

References

1. World Health Organization. *Global Status Report on Road Safety 2018, Licence: C*; World Health Organization: Geneva, Switzerland, 2018.
2. MacLeod, J.B.A.; Digiacomo, J.C.; Tinkoff, G. An evidence-based review: Helmet efficacy to reduce head injury and mortality in motorcycle crashes: EAST practice management guidelines. *J. Trauma Acute Care Surg.* **2010**, *69*, 1101–1111. [CrossRef] [PubMed]

3. Liu, B.C.; Ivers, R.; Norton, R.; Boufous, S.; Blows, S.; Lo, S.K. Helmets for preventing injury in motorcycle riders. *Cochrane Database Syst. Rev.* **2008**. [CrossRef] [PubMed]
4. Lin, M.R.; Kraus, J.F. A review of risk factors and patterns of motorcycle injuries. *Accid. Anal. Prev.* **2009**, *41*, 710–722. [CrossRef] [PubMed]
5. Kleiven, S. Why Most Traumatic Brain Injuries are Not Caused by Linear Acceleration but Skull Fractures are. *Front. Bioeng. Biotechnol.* **2013**, *1*, 15. [CrossRef] [PubMed]
6. Holbourn, A.H.S. Mechanics of head injuries. *Lancet* **1943**, *242*, 438–441. [CrossRef]
7. Ommaya, A.K.; Gennarelli, T.A. Cerebral Concussion and Traumatic Unconsciousness. *Brain* **1974**, *97*, 633–654. [CrossRef]
8. Gennarelli, T.A.; Thibault, L.E. Biomechanics of Acute Subdural Hematoma. *J. Trauma Inj. Infect. Crit. Care* **1982**, *22*, 680–686. [CrossRef]
9. Gennarelli, T.A.; Thibault, L.E.; Adams, J.H.; Graham, D.I.; Thompson, C.J.; Marcincin, R.P. Diffuse axonal injury and traumatic coma in the primate. *Ann. Neurol.* **1982**, *12*, 564–574. [CrossRef]
10. Lloyd, J.D. Biomechanics of Solo Motorcycle Accidents. *J. Forensic Biomech.* **2016**, *7*, 125. [CrossRef]
11. Chinn, B.; Canaple, B.; Derler, S.; Doyle, D.; Otte, D.; Schuller, E.; Willinger, R. COST 327 Motorcycle Safety Helmets. European Commission. Directorate General for Energy and Transport. 2001. Available online: https://ec.europa.eu/transport/road_safety/sites/default/files/pdf/projects_sources/cost327_final_report.pdf (accessed on 11 November 2021).
12. Bourdet, N.; Mojumder, S.; Piantini, S.; Deck, C.; Pierini, M.; Willinger, R. Proposal of a new motorcycle helmet test method for tangencial impact. In Proceedings of the IRCOBI Conference, Málaga, Spain, 14–16 September 2016; pp. 479–489.
13. Aldman, B.; Lundell, B.; Thorngren, L. Non-perpendicular impacts—An experimental study on crash helmets. In Proceedings of the IRCOBI Conference, Birmingham, UK, 8–10 September 1976.
14. Halldin, P.; Gilchrist, A.; Mills, N.J. A new oblique impacttest for motorcycle helmets. *Int. J. Crashworthiness* **2001**, *6*, 53–64. [CrossRef]
15. Aare, M.; Halldin, P. A new laboratory rig for evaluating helmets subject to oblique impacts. *Traffic Inj. Prev.* **2003**, *4*, 240–248. [CrossRef] [PubMed]
16. Pang, T.Y.; Thai, K.T.; McIntosh, A.S.; Grzebieta, R.; Schilter, E.; Dal Nevo, R.; Rechnitzer, G. Head and neck responses in oblique motorcycle helmet impacts: A novel laboratory test method. *Int. J. Crashworthiness* **2011**, *16*, 297–307. [CrossRef]
17. Mills, N.J.; Wilkes, S.; Derler, S.; Flisch, A. FEA of oblique impact tests on a motorcycle helmet. *Int. J. Impact Eng.* **2009**, *36*, 913–925. [CrossRef]
18. Bonugli, E.; Cormier, J.; Reilly, M.; Reinhart, L. *Replicating Real-World Friction of Motorcycle Helmet Impacts and Its Effects on Head Injury Metrics*; SAE Technical Paper 2017-01-1433; SAE International: Warrendale, PA, USA, 2017. [CrossRef]
19. Finan, J.D.; Nightingale, R.W.; Myers, B.S. The influence of reduced friction on head injury metrics in helmeted head impacts. *Traffic Inj. Prev.* **2008**, *9*, 483–488. [CrossRef] [PubMed]
20. Meng, S.; Fahlstedt, M.; Halldin, P. The effect of impact velocity angle on helmeted head impact severity: A rationale for motorcycle helmet impact test design. In Proceedings of the IRCOBI Conference, Athens, Greece, 12–14 September 2018; pp. 454–469.
21. Meng, S.; Cernicchi, A.; Kleiven, S.; Halldin, P. High-speed helmeted head impacts in motorcycling: A computational study. *Accid. Anal. Prev.* **2020**, *134*, 105297. [CrossRef] [PubMed]
22. Mills, N.J.; Gilchrist, A. Finite-element analysis of bicycle helmet oblique impacts. *Int. J. Impact Eng.* **2008**, *35*, 1087–1101. [CrossRef]
23. Ebrahimi, I.; Golnaraghi, F.; Wang, G.G. Factors influencing the oblique impact test of motorcycle helmets. *Traffic Inj. Prev.* **2015**, *16*, 404–408. [CrossRef]
24. Versace, J. *A Review of the Severity Index*; SAE Technical Paper 710881; SAE International: Warrendale, PA, USA, 1971. [CrossRef]
25. Takhounts, E.G.; Craig, M.J.; Moorhouse, K.; Mcfadden, J. Development of Brain Injury. *Criteria* **2013**, *57*, 243–266.
26. *ECE 22.06. Uniform Provisions Concerning the Approval of Protective Helmets and of Their Visors for Drivers and Passengers of Motorcycles and Mopeds*; UNECE Regulation: Geneva, Switzerland, 2021.
27. *FRHPhe-01. FIM Racing Homologation Programme for Helmets*; FIM: Mies, Switzerland, 2017.
28. Trotta, A.; Annaidh, A.N.; Burek, R.O.; Pelgrims, B.; Ivens, J. Evaluation of the head-helmet sliding properties in an impact test. *J. Biomech.* **2018**, *75*, 28–34. [CrossRef]
29. Ramalho, A.; Szekeres, P.; Fernandes, E. Friction and tactile perception of textile fabrics. *Tribol. Int.* **2013**, *63*, 29–33. [CrossRef]
30. Cua, A.B.; Wilhelm, K.P.; Maibach, H.I. Elastic properties of human skin: Relation to age, sex, and anatomical region. *Arch. Dermatol. Res.* **1990**, *282*, 283–288. [CrossRef] [PubMed]
31. Derler, S.; Rossi, R.M.; Rotaru, G.M. Understanding the variation of friction coefficients of human skin as a function of skin hydration and interfacial water films. *Proc. Inst. Mech. Eng. Part J J. Eng. Tribol.* **2015**, *229*, 285–293. [CrossRef]
32. Gerhardt, L.-C.; Strässle, V.; Lenz, A.; Spencer, N.; Derler, S. Influence of epidermal hydration on the friction of human skin against textiles. *J. R. Soc. Interface* **2008**, *5*, 1317–1328. [CrossRef] [PubMed]
33. Mills, N.J.; Gilchrist, A. Oblique impact testing of bicycle helmets. *Int. J. Impact Eng.* **2008**, *35*, 1075–1086. [CrossRef]
34. Trotta, A.; Zouzias, D.; de Bruyne, G.; Annaidh, A.N. The importance of the scalp in head impact kinematics. *Ann. Biomed. Eng.* **2018**, *46*, 831–840. [CrossRef]

35. Fahlstedt, M.; Halldin, P.; Alvarez, V.S.; Kleiven, S. Influence of the Body and Neck on Head Kinematics and Brain Injury Risk in Bicycle Accident Situations. In Proceedings of the IRCOBI Conference, Málaga, Spain, 14–16 September 2016; pp. 459–478.
36. Willinger, R.; Deck, C.; Halldin, P.; Otte, D. Towards advanced bicycle helmet test methods. In Proceedings of the International Cycling Safety Conference, Göteborg, Sweden, 18–19 November 2014.
37. Hering, A.M.; Derler, S. Motorcycle helmet drop tests using a hybrid iii dummy. In Proceedings of the IRCOBI Conference, Montpellier, France, 20–22 September 2000; pp. 307–321.
38. Ghajari, M.; Galvanetto, U.; Iannucci, L.; Willinger, R. Influence of the body on the response of the helmeted head during impact. *Int. J. Crashworthiness* **2011**, *16*, 285–295. [CrossRef]
39. Fahlstedt, M.; Abayazid, F.; Panzer, M.B.; Trotta, A.; Zhao, W.; Ghajari, M.; Gilchrist, M.D.; Ji, S.; Kleiven, S.; Li, X.; et al. Ranking and Rating Bicycle Helmet Safety Performance in Oblique Impacts Using Eight Different Brain Injury Models. *Ann. Biomed. Eng.* **2021**, *49*, 1097–1109. [CrossRef] [PubMed]